Revised Manuscript without Changes Marked
Click here to view linked References

Experimental study on thermal performance of porous phase change plates assisted air conditioning system in data centers

Zhongqiu Wang[a], Zujing Zhang[a]*, Xing Liang[b], Jiri Zhou[c], Hongwei Wu[d], Ruiyong Mao[a], Hongli Xu[a],
a College of Civil Engineering, State Key Laboratory of Public Big Data, Guizhou University, Guiyang 550025, China
b School of Computer Science and Mathematics, Kingston University London, KT1 2EE, United Kingdom
c China MCC5 Group CORP.LTD., MCC5 Tower, No. 9 Wuye Road, Jinjiang District, Chengdu, 610000, China
d School of Physic, Engineering and Computer Science, University of Hertfordshire, Hatfield, AL10 9AB, United Kingdom.
*Corresponding author: tel: +86 185 2391 9513 email: zjzhang3@gzu.edu.cn.

Abstract

The integration of phase change energy storage with cooling systems not only reduces the need for mechanical refrigeration in data centers (DCs), but also significantly enhances energy efficiency. However, research on the application location of phase change energy storage systems in DCs and the structural characteristics of system devices are limited. This paper combines the features of shell-and-tube and plate heat exchangers to design the porous phase change plate (PPCP) for use in DCs air conditioning systems and explores its cooling performance through experiments. The study employed single-factor and orthogonal experiments to analyze the effects of inlet air temperature, air velocity, aperture size and placement distance of the PPCP on the performance of the phase change heat device (PCHD) and evaluated the auxiliary effects of the device. The results indicate that: (1) The PCHD can reduce the air temperature by an average of 1.59 to 3.90 ℃ within 8 hours. (2) The aperture size of the PPCP significantly affects the cooling performance of PCHD: a reduction in the PPCP aperture size by 2 cm results in an 8% to 11% enhancement in cooling performance. (3) In a comprehensive analysis of multiple factors, the primary and secondary factors of the PPCP are inlet air temperature > air velocity > aperture size > placement distance. (4) During high-temperature loads, the PCHD can assist in reducing mechanical energy consumption by up to 63%.

Keywords

Porous phase change plates； Phase change heat device; Data centers; Energy saving; Air conditioning system.

Nomenclature

T	Temperature, °C
P	Cooling power, W
Q	Refrigeration capacity, J
△T	Temperature difference，°C
m	Mass, kg
Greek symbols	
α	Domain value
γ	Liquid volume fraction
η	Energy saving rate
μ	Total uncertainty
λ	Efficiency
τ	Time
Subscripts	
T_{PCM}	Temperature of PCM, °C
T_{ij}	Temperature of the measuring point, °C
x_i	Abscissa of the measurement point
y_j	Ordinate of the measurement point
T_{in}	Temperature of inlet air, °C
T_{out}	Temperature of outlet air, °C
T_s	Temperature of phase change materials begin to melt, °C
T_l	Temperature of fully melted phase change materials, °C
T_a	Temperature of standard supply air temperature, °C
S_{pcm}	PCM area, m^2
S_{total}	Total area, m^2
V_a	Velocity of outlet air, m/s
A_a	Ventilation surface area, m^2
P_w	Input power, W
ρ_a	Density of air, kg/m^3
c_p	specific heat, J/(kg·K)
Acronyms	
PCM	Phase change material
PPCP	Porous phase change plate
PCHD	Phase change heat device
DC	Data center
TES	Thermal energy storage
COP	Coefficient of performance

1 Introduction

In recent years, the scale of data centers (DCs) has been expanding with the growing demand for DC services [1-3]. In 2024, DCs consumed about 415 terawatt-hours (TWh) of electricity, accounting for approximately 1.5% of global electricity consumption [4]. It is expected that by 2030, the power consumption of DCs is projected to double compared to 2024 levels [5], leading to a direct or indirect increase in carbon emissions. With the advent of the digital era, DCs is expected to account for over 14% of global emissions by 2040 [6]. However, to ensure the safe and stable operation of DCs, the cooling systems must operate continuously [7, 8]. This heavy reliance on energy consumption accounts for 30% to 50% of total power usage [9-12]. The high electricity demand of cooling systems, which depend on fossil fuels like coal and natural gas, leads to substantial carbon emissions that exacerbate global warming. Depending on the size and load of the DC, the energy consumption and efficiency of the cooling system determine the total energy consumption [13-15]. Therefore, improving cooling performance and energy efficiency with existing technologies is critical to reducing energy demand and reducing carbon emissions.

Among the existing energy saving and environmental protection technologies, one of the effective ways to reduce energy consumption is natural cooling. Natural cooling technology is a kind of green energy saving technology which uses natural cold sources and has great energy saving potential [16, 17]. In particular, the air-cooling system that takes advantage of natural freezing air is widely used in DCs [18]. The system utilizes natural freezing air for equipment heat dissipation, thereby reducing operational costs, saving energy, and minimizing environmental impact.[19]. Silva-Llana et al. [20] compared the natural cooling system with the traditional system model. The results show that the air side natural cooling is feasible and effective in DCs. Jahangir et al. [21] examined the importance of natural cooling technology and found that the combination of natural cooling systems with renewable energy has great potential. Although natural cooling technology holds significant potential for energy savings and emission reduction, its cooling source supply is subject to seasonal and environmental fluctuations, resulting in intermittent availability [22, 23]. This variability creates spatiotemporal challenges for practical implementation. At present, the reasonable application of energy storage technology in various fields has become a research hotspot to improve energy efficiency [24]. Among them, thermal energy storage (TES) has emerged as a pivotal technology for cooling systems, effectively bridging temporal, thermal, and spatial gaps in energy supply-demand[25]

TES can be divided into sensible heat storage, latent heat storage and chemical energy storage[26], Latent heat energy storage is to use phase change materials (PCMs) to absorb and release latent heat to store energy [27], with high energy storage density, stable temperature fluctuation, energy saving and environmental protection characteristics, which is widely been used [28-30]. Huang et al. [31] proposed a top air conditioning system with TES. The study shows that the heat storage system can meet the cooling requirements of 5 min emergency cooling under all working conditions. Yan et al. [32]designed a new sandwich spiral structure for a solar phase change heat storage system for residential applications. The study shows that the energy efficiency of the system is 38.5%, and the exergy efficiency is 8.3%. Yang et al. [33] proposed a new cooling system that combined direct ventilation cooling with phase change energy storage. The results showed that the cooling capacity could reach 2.19×10^4 kJ within 8 hours. Yi et al. [34] designed a cooling system that integrates evaporative cooling with phase change energy storage. The findings indicate that the integrated cooling unit can reduce the air temperature by 10 °C–3 °C in 8 h. However, there is still a research blank concerning detailed optimization and continuous utilization of TES.

Recent years, more researchers have begun to use composite materials, optimization of structure and other methods to improve the performance of phase change devices [35-39]. Li et al. [40] studied the heat behavior of plate phase change heat devices (PCHD) under ventilation conditions. It was found that the ventilation flow, ambient temperature, and humidity all contributed to enhanced heat transfer increased heat transfer. Ahmadi et al. [41] used numerical simulation technology to investigate the effect of spiral tube diameter and pipe diameter on the performance of phase change energy storage equipment. The study found that the spiral tube diameter was more important to the energy storage process than the pipe diameter. Ma et al. [7] designed an integrated shell-and-tube latent heat storage system emergency cooling system for the rapid cooling of DCs. Results showed that the developed cooling device can provide continuous cooling protection for servers in operation for approximately 6 minutes. Giorgio et al. [42] investigated the novel class of pillow-plate latent heat thermal energy storage systems based on the combined use of PCM of pillow plate heat exchanger technology. The study shows that demonstrated superior thermal and economic performance, reducing the required heat exchange area and lowering both energy and power capacity costs. Zhang et al. [43] proposed a branch type heat sink design suitable for shell and tube heat exchangers. The study showed that compared with the traditional longitudinal heat sink, this branch type heat sink has excellent performance in enhancing heat storage.

In summary, previous studies have explored the application of phase change thermal energy transfer combined with natural cooling sources. The primary applications in DCs are plate structures for air cooling and shell-and-tube structures for liquid cooling. However, in air cooling systems, plate structures often suffer from insufficient and uneven internal heat exchange. To overcome the limitations of traditional plate-shell phase-change heat exchangers, this paper designs a porous phase change plate (PPCP) heat exchanger for thermal management in air conditioning systems. To address the challenges of inadequate heat transfer and uneven distribution in conventional flat-plate air cooling systems. Simultaneously, a modular design approach is adopted to avoid the complex integration characteristics of shell-and-tube configurations. This innovation ensures that phase-change devices maintain their heat exchange performance while improving flexibility and operational convenience.

This study, based on the characteristics of plate and shell-and-tube structures, considering the internal structure of air conditioning systems, designed the PPCP heat exchanger. The effects of inlet air temperature, air supply velocity, aperture size, and the placement of PPCP on the performance of the device is investigated. The experiments confirm the thermal performance superiority of the porous architecture over traditional plate designs, establishing this PPCP heat exchanger as a promising candidate for next-generation cooling applications.

2 Methodology

2.1 Principle of the PCHD assisted air conditioner for data centers

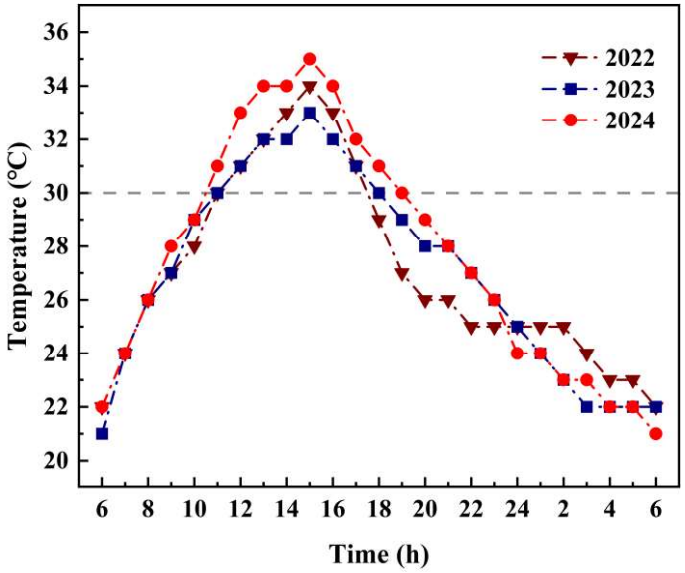


Fig. 1. The full-time temperature of the highest day of the year.

As an important hub for the development of DCs, Gui'an District of Guizhou Province, China, boasts unique climatic advantages. Figure 1 shows the variation in temperature during the hottest days from 2022 to 2024, with diurnal temperature differences typically exceeding 10 ℃ and temperatures above 30 ℃ lasting about 8 hours. Considering the low annual average temperature and significant diurnal temperature variations in Gui'an District, utilizing wind cooling and phase change energy storage systems to assist air conditioning is an effective way to conserve resources.

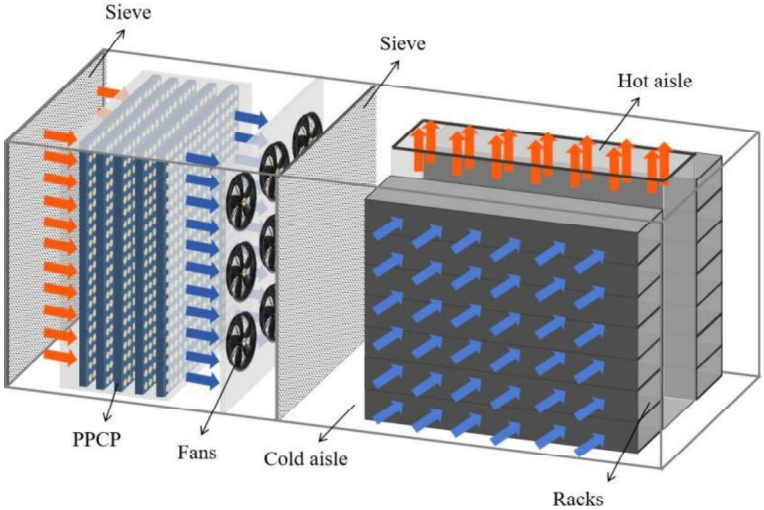


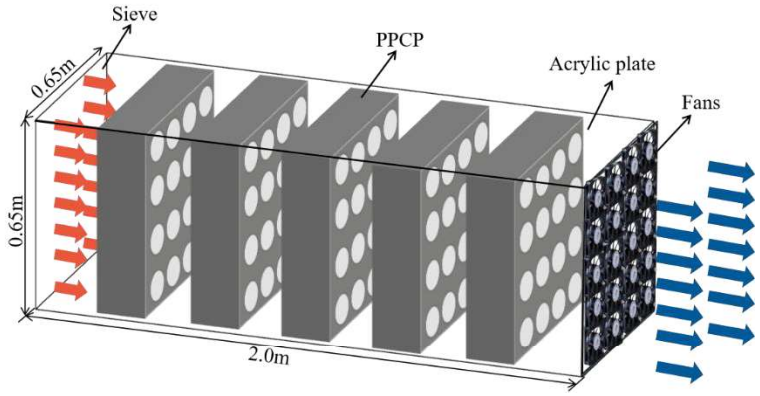
Fig. 2. Phase change assisted operation schematic diagram.

As a critical component of DC cooling systems, air conditioning systems are widely employed due to their independent operation and ease of installation. When climatic conditions are favorable, direct cooling using outside air can effectively reduce energy consumption. However, when ambient air conditions cannot meet the cooling demands of DCs, this study integrates phase change energy storage technology into the air conditioning system by adding the PCHD within the system to reduce reliance on mechanical cooling. As illustrated in Figure 2, the schematic diagram of the operating principle of the phase change heat exchange section in a DC is presented. During periods of low

ambient temperature, cool air enters the air conditioning system, where cooling energy is stored by solidifying the PCM via PCHD. During periods of high temperature, as the outdoor air temperature rises, outside air enters the system and transfers heat with the PCM through the PCHD, thereby lowering the supply air temperature. After this process, the treated air meets the supply requirements, passes through ordered filtration, and enters the data hall for heat exchange with the servers, eventually being discharged through a sealed hot aisle.

2.2 Overview of the experimental PCHD

2.2.1 Experimental model



(a)



(b)



(c)

Fig. 3. PCHD structure diagram.

(a) PCHD schematic; (b) PCHD physical diagram; (c) Three types of PPCPs.

Figure 3 shows the structure of the PCHD, which features a shell made of 5 mm thick transparent acrylic and an internal channel measuring 2 m in length, 0.65 meters in width, and 0.65 m in height. The PPCP uses a 1 mm thick stainless-steel shell with dimensions of 0.64 m in length, 0.20 m in width, and 0.60 m in height. The packaging boards are designed and processed with three aperture

sizes: 6 cm, 8 cm, and 10 cm, preparing five pieces for each size and ensuring the same α value for each type. The PPCP sits inside the ventilation duct. Twenty small fans, arranged in five rows and four columns, deliver uniform airflow by the adjustment knob.

2.2.2 Experimental materials

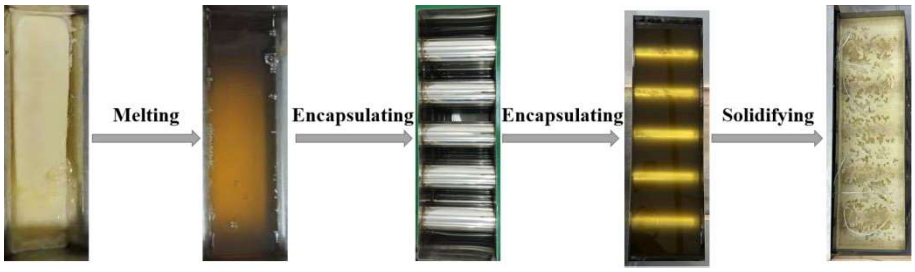


Fig. 4. The encapsulation process of PPCP.

Table 1
Material properties

Material (Paraffin)	
Starting temperature of melting (˚C)	25.12/29.04
Starting temperature of solidification (˚C)	23.79/22.94
Density(kg/m^3)	880
Thermal conductivity (W/ (m·K))	0.21
Latent heat (kJ/kg)	165.9/168.9
Specific heat (kJ/ kg·K)	3.22

Considering the meteorological conditions in Gui'an District, Guizhou, with an average summer temperature of about 23.5°C, requiring a material with low phase transition temperature and high latent heat characteristics. Since they are used in data centers, the material needs to be non-corrosive and capable of withstanding overheating without decomposition. Compared to other phase change materials, paraffin demonstrates superior thermal stability, reversible thermal cycling, and safety, showing significant advantages in renewable energy integration applications [44]. In addition, the melting point range of paraffin wax can be adjusted, so paraffin wax with phase transition temperature between 23-25°C is selected as the experimental material to make full use of its latent heat storage and release characteristics in summer. As shown in Figure 4, the paraffin wax is melted into a liquid and filled into PPCP for encapsulation. Table 1 lists the thermophysical properties of experimental materials.

2.3 Experimental principle of the PCHD

2.3.1 Experimental platform

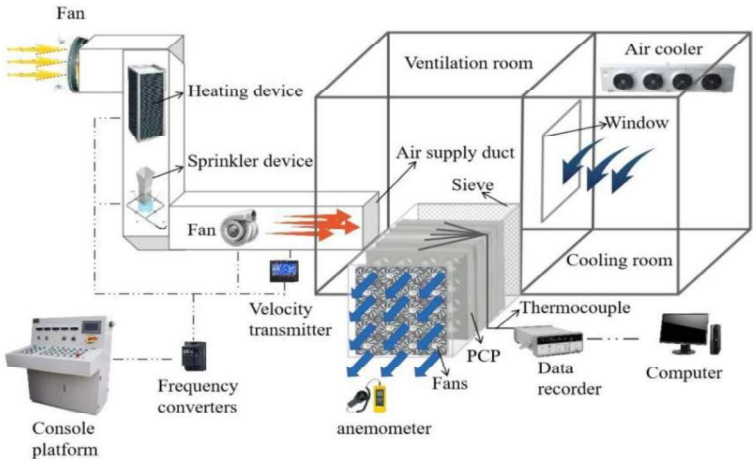


Fig. 5. Schematic diagram of the experimental principle

Figure 5 shows that, under simulated daytime conditions, ambient air is drawn into the treatment system by centrifugal fans, while the control platform dynamically modulates airflow parameters to maintain different air status. Then the heated air is sent into the ventilation room through the supply ducts of the fan section. Assisted by a fan wall composed of small fans, the air flows into the PCHD for temperature regulation. Under simulated nighttime air conditions, the air cooler cools the air before sending it to the ventilation room. The fan wall then directs the air into the PCHD for cooling.



Fig. 6. Experimental platform diagram

Figure 6 shows that the experimental platform is in the Artificial Environment Laboratory of Guizhou University. The experimental platform includes a simulated environmental device and the PCHD. The simulated environmental device primarily consists of a ventilation room. The left side of the ventilation room connects to the air handling ducts, which include heating, spraying, and air supply equipment. The right side connects to a cooling chamber through a window that is 1.1 meters long and 0.9 meters wide. The front side connects to the PCHD.

2.3.2 Data acquisition



(a) (b) (c) (d)

Fig. 7. Experimental instruments diagram.
(a) Data acquisition logger; (b) Anemometer; (c) Fan; (d) Thermal resistance.

Table 2
Main design parameters of instrument.

Equipment name	Equipment type	Uncertainty	Range
Data acquisition logger	JK4000	Read value × 0.5 %± 0.5 ℃	− 200 ~ 200 ℃
Fans	SF8025AT	± 0.05 m^3/ min	2 m^3/ min
Thermal resistance	PT1000	± 0.01 ℃	− 50 ~ 100 ℃
Airflow Anemometer	FLUKE-925	±0.05 m/s	0.50~5.00 m/s

The main instruments of the experiment include variable speed fans, PT1000 thermal resistance, data acquisition instrument and anemometer. The photos of the experimental equipment are shown in Figure 7, and the main technical parameters are shown in Table 2.

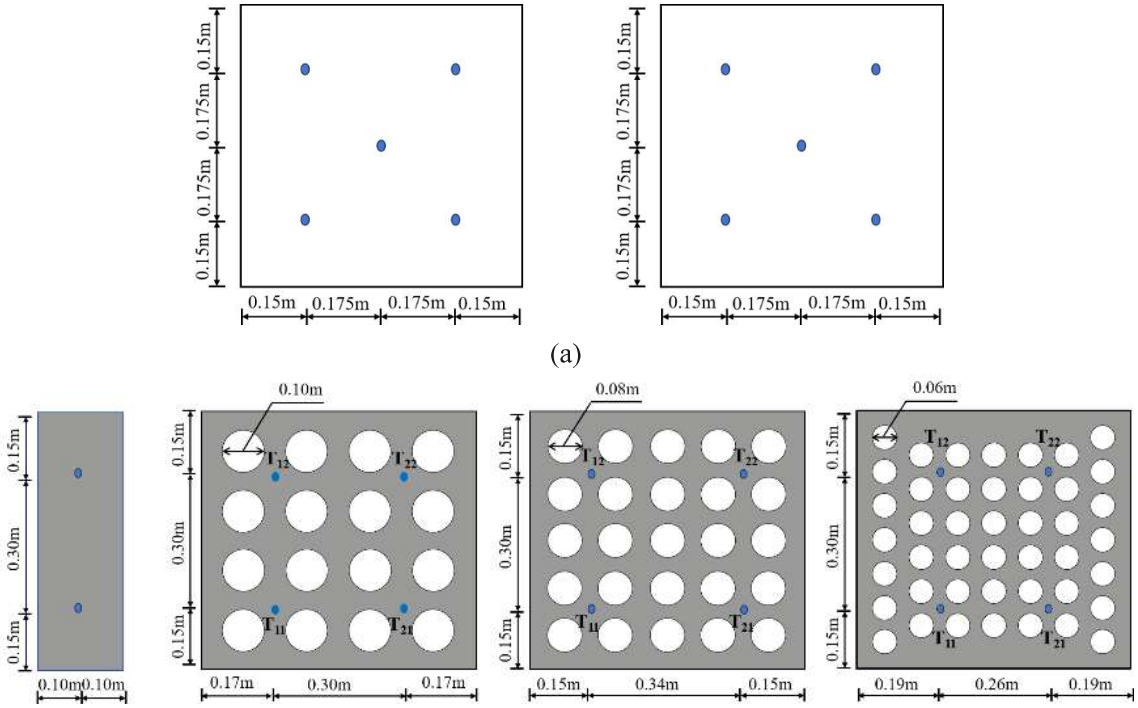


Fig. 8. Layout of temperature measuring points.
(a) Inlet and outlet of the PCHD; (b) Inside of the PPCP.

Figure 8 shows the layout of the PCHD measurement points. Figure 8(a) shows that five PT1000 thermistors are installed at each end of the device to measure the inlet and outlet air temperatures. The front measurement point is located 5 cm behind the filter, while the rear measurement point is 10

cm away from the exhaust port. Figure 8(b) shows four measurement points set inside the PPCP. In the experiment, a handheld anemometer is used to measure the wind speed at 25 cm from the fan wall. To ensure the accuracy of the experiment, all experimental equipment is calibrated after installation and connection, the PT1000 thermistor is also calibrated. Thermistors are connected to the data acquisition system to record all temperature readings in real time. During the experiment, the data acquisition system records temperature sensor readings every two minutes and transmits all temperature data to the computer for further processing.

2.3.3 Design of experimental cases

Taking the meteorological data from Gui'an District in Guizhou Province as an example, this study aims to optimize the design of PCHD to absorb heat more efficiently from the air and assist the air conditioning system in cooling. In the experiment, ensuring the stability and continuity of airflow at the equipment inlet is crucial for the reliability of the experimental results. The inlet temperature refers to the air temperature entering the PCHD, whereas the supply air temperature denotes the conditioned air temperature at the discharge terminal after thermal processing. The wind speed is the air velocity passing through the fan wall. This experiment focuses on the impact of four parameters on system performance: the inlet air temperature, the air velocity, the aperture size of the PPCPs, and the distance between the PPCPs.

Over the past three years, the highest temperature recorded in the Gui'an District has been 34.95 ℃. Considering global warming and the potential for extreme heat, the upper limit for the designed temperature is set at 36 ℃. Taking a data center in Gui'an New Area using air conditioning systems as an example, the supply air temperature in its server room is set between 23 °C and 27 °C and the air supply velocity is 0.82 m/s-2.39 m/s, and the air speed was found to be effective between 1.5 and 3 m/s during the experimental test[33]. Therefore, the experimental inlet air temperature range is set between 27 ℃ and 36 ℃ and the air velocity is set between 1 m/s and 2.5 m/s. The ratio of PCM space to area is defined by the value of α. Under the same α-value, the heat transfer performance of different pore sizes is investigated. As previous studies [45] have investigated 4 cm and 12 cm aperture sizes, three packaging plates with three aperture sizes (6 cm, 8 cm and 10 cm) are set up in this experiment. At the same time, the length of each functional section of the air conditioning unit is about 1 m-2 m, therefore, the spacing of the plates is set to 0 cm, 5 cm, 10 cm, and 15 cm. The required length range of PCHD is 1-1.6 m to match the size of the air conditioning unit. As shown in Figure 9, four PPCP placement distances are designed.

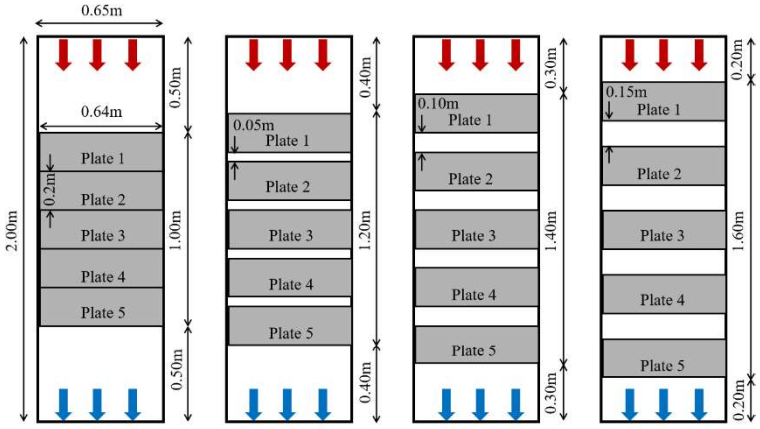


Fig. 9. PPCPs placement diagram

Through a single-factor experimental analysis, the study investigated the impact of specific factors on the performance of phase change thermal storage devices. The inlet air temperature, air

velocity, aperture size of the PPCPs, and the placement distance of the PPCPs were examined, with only one factor altered at a time while the others remained constant. Table 3 presents the parameters for each single factor.

Table 3

Design of single-factor experiment.

Case	Inlet air temperature (°C)	Velocity (m/s)	Aperture (cm)	Distance (cm)
1	33	1.5	10	0
2	27	1.5	10	0
3	30	1.5	10	0
4	36	1.5	10	0
5	33	1.0	10	0
6	33	2.0	10	0
7	33	2.5	10	0
8	33	1.5	8	0
9	33	1.5	6	0
10	33	1.5	10	5
11	33	1.5	10	10
12	33	1.5	10	15

As the influencing factors change, the equipment system will also be adjusted accordingly, which will affect its cooling performance. Therefore, this study further optimized the cooling performance of PCHD using the orthogonal experimental method, focusing on four parameters that affect the system's cooling effect in environments above 30 °C with limited space requirements: inlet air temperature, air velocity, aperture size of the PPCPs, and placement distance of the PPCPs. Through orthogonal analysis, the primary and secondary effects of these factors can be determined. This study employed four influencing factors, each with three levels. A total of nine experimental groups were conducted. For more detailed information, please refer to Table 4 below.

Table 4

Orthogonal experimental table $L_9(3^4)$.

Case	Inlet air temperature (°C)	Velocity (m/s)	Aperture (cm)	Distance (cm)
13	30	1.5	10	0
14	33	2.5	10	5
15	36	2	10	10
16	36	2.5	8	0
17	30	2.0	8	5
18	33	1.5	8	10
19	33	2	6	0
20	36	1.5	6	5
21	30	2.5	6	10

2.3.4 Experimental process

The experiment changes the arrangement of PPCP by changing the distance between them, and the internal device changes it by replacing the packaging structure of different apertures. In addition, the temperature working range of the whole experimental condition is 27 ~ 36 °C, and the air speed range is 1 m/s ~ 2.5 m/s. Take experimental case 1 as an example.

The following section details the experimental process.

(1) 10 cm PPCPs are placed without intervals in a channel 30 cm away from the air inlet of the

device, and the thermocouple is connected to the data recorder.

(2) Activate the data logger and set the recording interval to 2 min.

(3) Start the air cooler, blow freezing air into the ventilation room, induce PCM cooling and curing and maintain the device temperature at 22 ± 0.5 ℃.

(4) Turn off the air cooler, start the controllable constant temperature air supply system, and the air temperature at the air inlet is stable at 33 ± 0.5 ℃.

(5) Start the fan, adjust the wind speed, and control the wind speed of the air inlet to 1.5 ± 0.2 m/s.

(6) After the experiment lasts for 8 hours, turn off the controllable constant temperature air delivery system, extract the temperature data from the data acquisition recorder, and analyze it.

(7) Repeat the above steps and change the packaging structure, arrangement, and parameters according to different experimental cases until all experimental cases are completed.

To ensure the effectiveness and accuracy of the experiment, it is crucial to keep the initial temperature of the system device within the same range before each experimental case begins.

2.4 Data processing

2.4.1 Evaluation index

α can be defined as the ratio between the PCM space and the domain. The calculation method of the α is as follows [46]:

$$\alpha = \frac{S_{pcm}}{S_{total}} \quad (1)$$

Where: S_{pcm} is the region of PCM, S_{total} is the overall region.

The surface of PPCP is divided into 1 cm^2 grids, and multiple measurement points are arranged to obtain the temperature of each measurement point. According to the temperature of each measurement point, the temperature of each grid is obtained by linear interpolation, to deduce the liquid phase variation law of PCM. The calculation method of T_{PCM} is as follows [40]:

$$f(T_{pcm}) = \frac{f(T_{11})}{(x_2-x_1)(y_2-y_1)}(x_2-x)(y_2-y) + \frac{f(T_{21})}{(x_2-x_1)(y_2-y_1)}(x-x_1)(y_2-y) + \frac{f(T_{12})}{(x_2-x_1)(y_2-y_1)}(x_2-x)(y-y_1) + \frac{f(T_{22})}{(x_2-x_1)(y_2-y_1)}(x-x_1)(y-y_1) \quad (2)$$

Where: T_{PCM} is the temperature of the PCP (°C), T_{ij} is the temperature of the measurement point (°C), x_i and y_j are the coordinates of the measurement point in the PPCP.

The calculation method of the μ is as follows[7]:

$$\gamma = \begin{cases} 0 & T_{pcm} \le T_s \\ \frac{T_{pcm}-T_s}{T_l-T_s} & T_s < T_{pcm} < T_l \\ 1 & T_{pcm} \ge T_l \end{cases} \quad (3)$$

Where: T_s is the solid phase temperature of PCM (°C), T_l represents the liquid phase temperature of PCM (°C).

The temperature difference is a visual reflection of the cooling capacity of the device. The calculation method of the $\triangle T$ is as follows:

$$\Delta T(t) = T_{in}(t) - T_{out}(t) \quad (4)$$

Where: T_{in} is the temperature of inlet air (°C), T_{out} is the temperature of outlet air (°C).

The cooling power is determined according to the air flow and temperature at the inlet and outlet, which reflects the heat transfer rate during the phase change process. The calculation method of the P is as follows [47]:

$$P = \rho_a V_a A_a c_p [T_{in}(t) - T_{out}(t)] \quad (5)$$

Where: ρ_a is the air density (kg/m^3), V_a is the air velocity (m/s), A_a is the air circulation area (m^2), c_p is the specific heat of the air J/(kg·K).

Effectiveness expresses the thermal performance of the unit regarding its maximum cooling potential. The effectiveness depends on the temperature of the air at the inlet and outlet of the unit and the initial temperature of the system. The calculation method of the λ is as follows [48]:

$$\lambda = \frac{P}{P_{max}} = \frac{\rho_a V_a A_a c_p (T_{in}(t) - T_{out}(t))}{\rho_a V_a A_a c_p (T_{in}(t) - T_{init})} = \frac{T_{in}(t) - T_{out}(t)}{T_{in}(t) - T_{init}} \quad (6)$$

Where: T_{inti} is the PCM initial temperature (°C), P_{max} is the maximum cooling power (W).

The overall heat absorbed by PCHD reflects the heat load it bears per unit time. The calculation method of the Q is as follows [49]:

$$Q = \int_0^t \rho_a V_a A_a c_p [T_{in}(t) - T_{out}(t)](t) dt \quad (7)$$

The PCHD assists in saving mechanical refrigeration energy consumption, reflecting the overall energy-saving level of the system by the device. The calculation method of the η is as follows [33]:

$$\eta = \frac{\sum_{i=1}^{n} (T_{in}(t) - T_a)\tau_i - \sum_{i=1}^{n} (T_{in}(t) - T_a - \Delta T(t))\tau_i}{\sum_{i=1}^{n} (T_{in}(t) - T_a)\tau_i} \times 100\% \quad (8)$$

Where: T_a is the standard air supply temperature (°C), τ_i is the mechanical cooling time (h).

The energy efficiency level directly reflects the PCHD's ability to utilize energy. The calculation method of the COP is as follows [50]:

$$COP = \frac{P}{P_w} \quad (9)$$

Where: P_w is the input power (W).

2.4.2 Error analysis

The measurement uncertainty values of the variable-speed fan, PT1000 RTD, data acquisition instrument, and anemometer used in this experiment are shown in Table 2. In addition, there are uncertainties in measuring temperature, wind velocity, and weight.

$$\mu = \pm \sqrt{\left(\frac{\Delta T_D}{T_D}\right)^2 + \left(\frac{\Delta T_T}{T_T}\right)^2 + \left(\frac{\Delta V_A}{V_A}\right)^2 + \left(\frac{\Delta V}{V}\right)^2 + \left(\frac{\Delta T}{T}\right)^2 + \left(\frac{\Delta m}{m}\right)^2} \times 100\% \quad (10)$$

Table 5

Uncertainty of measurement and instrument parameters.

Items		Uncertainty
Thermal resistance	$\triangle T_T / T_T$	1.25%
Data acquisition logger	$\triangle T_D / T_D$	1.75%
Airflow anemometer	$\triangle V_A / V_A$	2%
Wind velocity	$\triangle V / V$	3%
Temperature	$\triangle T / T$	1.6%
Weight	$\triangle m / m$	1.1%

The uncertainty values of the measuring devices used in the experiments are given in Table 5. The results are derived from (10) [51], and the overall uncertainty of the experimental system is 4.62%.

The primary sources of experimental errors in this study originate from inherent instrument uncertainties. The thermal resistance, data acquisition recorder, and anemometer used in the experiment have respective uncertainty levels of 1.25%,1.75%, and 2%. To minimize instrument-related errors, we recommend upgrading higher-precision thermal resistors and data acquisition devices, while ensuring thorough calibration of the anemometer prior to use. Then, measurement errors may occur during wind speed and temperature measurements. To mitigate these, multiple measurement points should be established with repeated sampling. Additionally, environmental factors significantly impact experimental accuracy. As weather changes and seasonal variations affect temperature and humidity levels throughout the experiment, monitoring and controlling surrounding environmental conditions is essential to reduce such interference.

3 Results

3.1 Thermal characteristics of PPCPs

3.1.1 Cold storage process

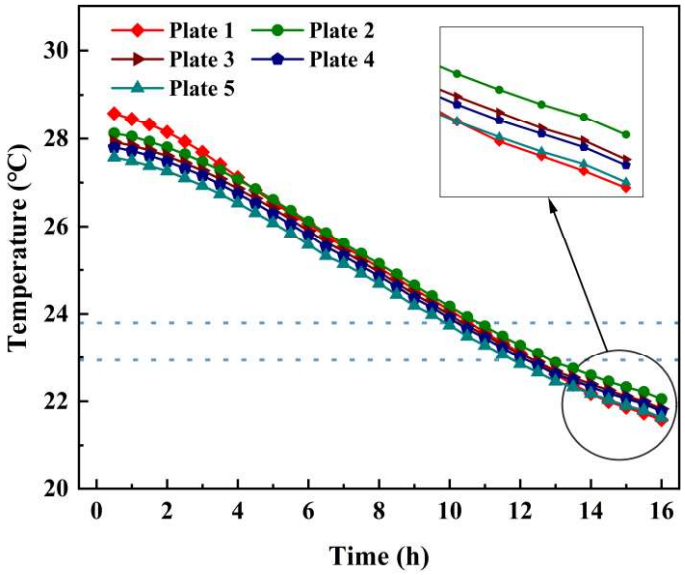
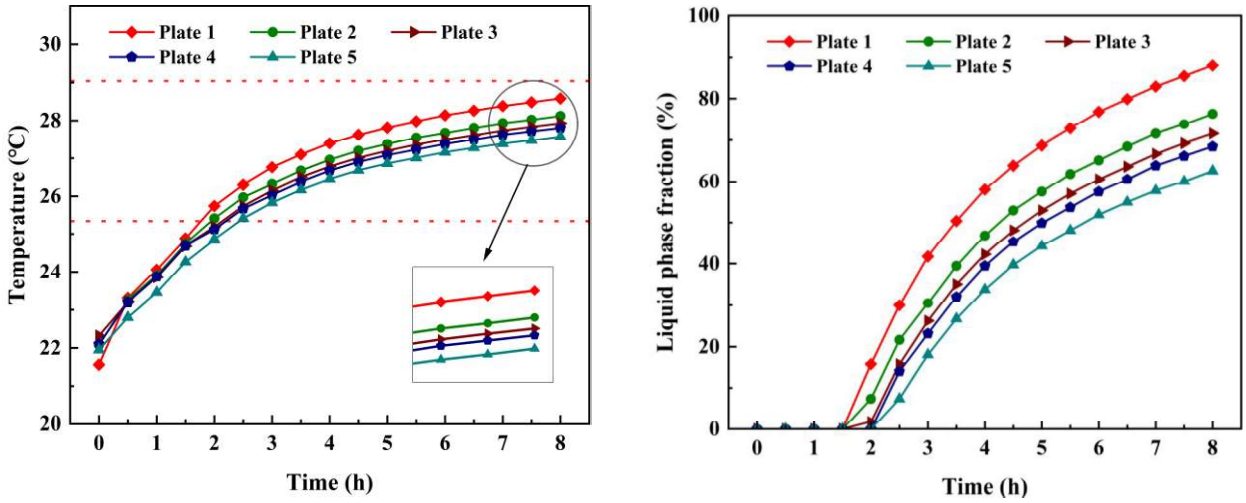


Fig. 10. Temperature of PPCP during cold storage.

Figure 10 shows the PCHD using plates with the aperture size of 8 cm, placed in the channel without any distances, at inlet air temperature of 21 °C to 26 °C and air velocity of 1.5 m/s, subjected to 16 hours refrigeration process. It can be seen that the temperature of the PPCPs gradually decreases over time, and the five plates show a similar trend. Compared to the other boards, Board 1, which comes into contact with a cold source faster, experiences a quicker rate of temperature decline. According to the material properties, PCM is fully cured at 22.94 °C, PPCP is completely cured after 13 hours, and the temperature is about 22 °C after 16 hours.

3.1.2 Heat absorption process



(a) (b)

Fig. 11. The heat absorption process of PPCP:(a) Temperature of PPCP. (b) Liquid phase fraction of PPCP.

Figure 11 (a) shows the PCHD using plates with the aperture size of 8 cm, placed in the channel without any distances, at inlet air temperature of 36 °C and air velocity of 2.5 m/s, subjected to 8 hours heat absorption process. The PPCPs begin to absorb heat at an initial temperature of 22°C±0.5°C, and the temperature rises over time, although the heating rate gradually slows down. Additionally, Plate 1, which comes into contact with the heat source more quickly during the temperature change, experiences a faster internal temperature increase compared to the other plates. (b) shows the changes in the liquid phase fraction of PPCPs during the heating process. It is evident that within the first 2 hours, PPCPs primarily undergo sensible heat exchange, with the liquid phase fraction remaining stable. From 2 to 8 hours, the PPCPs undergo latent heat exchange, leading to a gradual increase in the liquid phase fraction over time. After 8 hours, the liquid phase fraction of PPCPs exceeds 60%, resulting in a partial loss of cooling capacity.

3.2 Refrigeration capacity of the PCHD

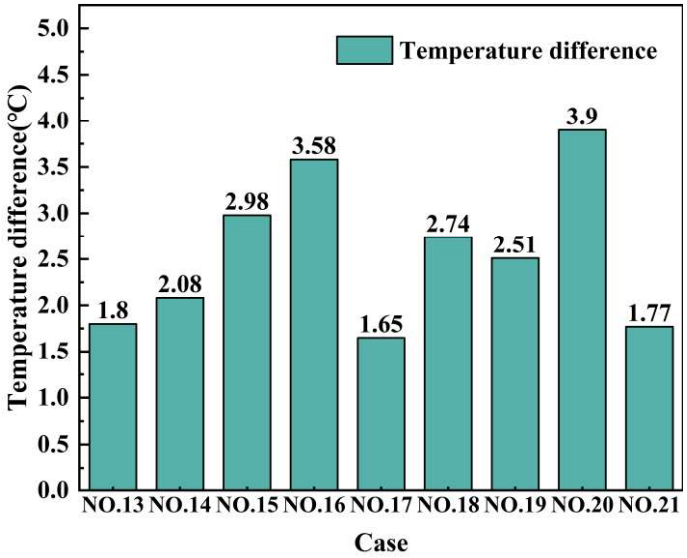


Fig. 12. The average temperature difference of the orthogonal experiment.

Figure 12 shows the average temperature difference between inlet and outlet of 9 orthogonal experimental heat absorption processes within 8 hours. The PCHD can reduce the average air

temperature by 1.65~3.9 °C within 8 hours in the high temperature environment above 30 °C, among which the maximum temperature difference between inlet and outlet is 5.03 °C when the inlet air temperature is 36 °C.

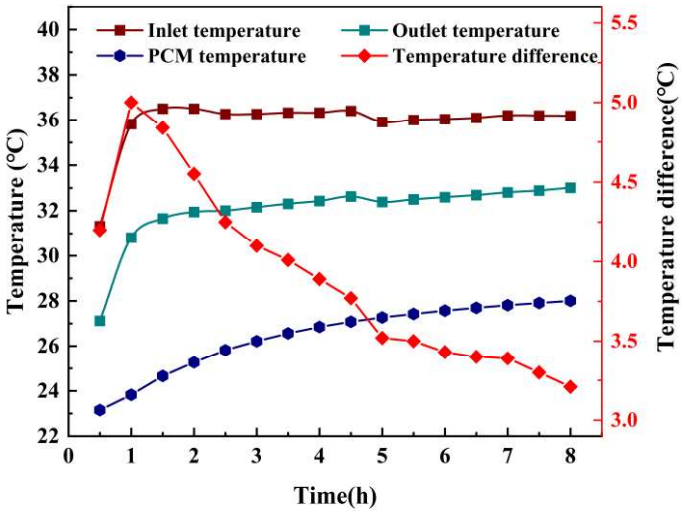


Fig. 13. The PCHD during the heat absorption process.

Figure 13 shows the changes in inlet air temperature, outlet air temperature, PCM temperature, and temperature difference under case 20 conditions. As the inlet air temperature rises to around 36 °C, both the outlet and PCM temperatures also gradually increase. In the first 2.5 hours, the inlet and outlet temperatures peak at 5.03 °C before rapidly declining. This is due to the initial sensible heat exchange, which causes significant temperature fluctuations. After 2.5 hours, the PCHD switches to latent heat exchange, resulting in smaller temperature fluctuations and a gradual decline. After an 8-hour heat exchange process, the temperature difference of the PCHD remains above 3 °C, with the entire process reducing the air temperature by an average of 3.9 °C, demonstrating excellent heat exchange performance.

3.3 Sensitive analysis

3.3.1 Effect of the aperture size

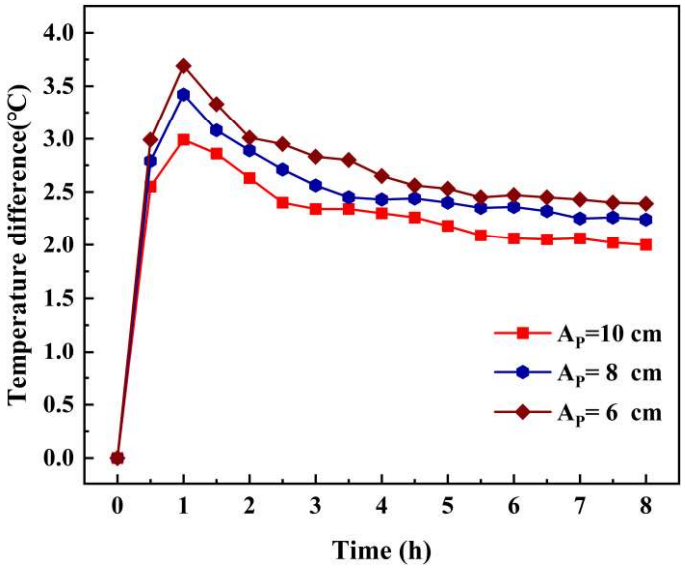


Fig. 14. Temperature difference profiles at different aperture sizes.

Figure 14 shows the device placed without distance, with the inlet air temperature of 33 °C and

the air velocity of 1.5 m/s. The variation of temperature difference over 8 hours under different aperture sizes shows that as the aperture size decreases, the temperature difference increases. This is due to the decrease in aperture size leading to an increase in heat transfer area, thereby enhancing the contact interface between air and PCMs. Under the same amount of PCMs, as the aperture decreases, the temperature difference gradually increases. When using the aperture size of 6 cm, the maximum temperature difference reaches 3.69 ℃. The average temperature differences for aperture sizes of 10 cm, 8 cm, and 6 cm within 8 hours are 2.30 °C, 2.55 °C, and 2.75 °C. As the aperture size decreases from 10 cm to 8 cm, the average cooling temperature increases by 0.20 ℃, and the cooling performance is enhanced by 8%. As the aperture size decreases from 8 cm to 6 cm, the average cooling temperature increases by 0.25℃, and the cooling performance is enhanced by 11%.

3.3.2 Effect of the placement distance

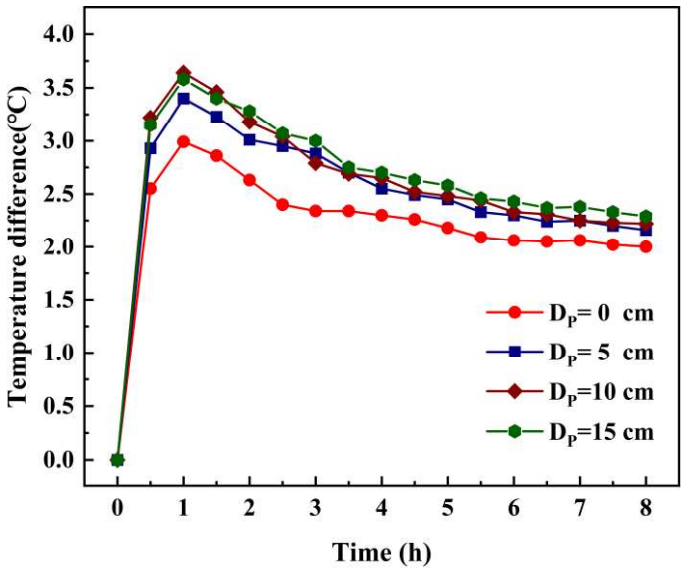


Fig. 15. Temperature difference profiles at different placement distances.

Figure 15 shows the device placed without distance, with the inlet air temperature of 33 ℃ and the air velocity of 1.5 m/s. 8 hours temperature difference variation under different aperture sizes. In contrast, the temperature difference is smaller when placed without any distance. This is because compared to placement with spaced distances, spaced placement has a larger heat transfer area, thereby improving heat exchange efficiency. Among the four different placement distances, the performance is significantly worse when placed without a gap, while the effect is similar for distances of 5 cm, 10 cm, and 15 cm. The average temperatures within 8 hours for four different placement distances are 2.32 ℃, 2.65 ℃, 2.72 ℃, 2.78 ℃.

3.3.3 Effect of the inlet air velocity

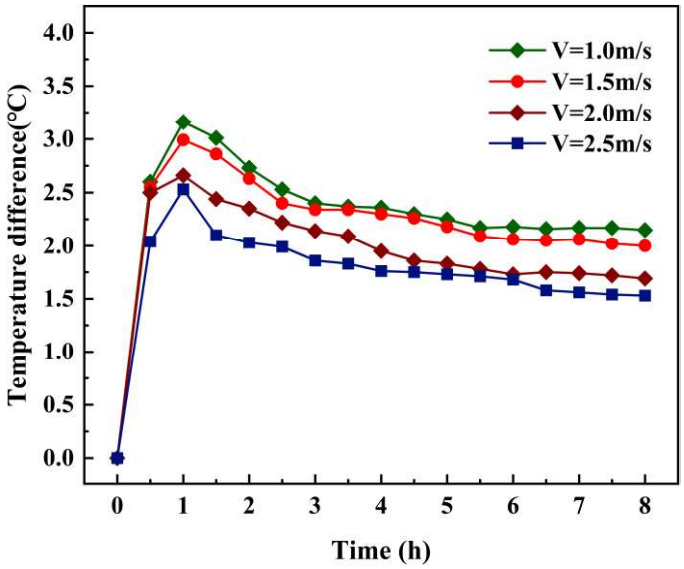


Fig. 16. Temperature difference profiles at different air velocities.

Figure 16 shows the device placed without distance, with the inlet air temperature of 33 ℃ and the aperture size of 10 cm. The temperature difference changes over 8 hours at different air velocities. As the air velocity increases, the temperature difference decreases. This is mainly due to the increase in air velocity, which leads to an increase in the amount of air supplied per unit time, thereby reducing the residence time of air on the heat exchange surface and shortening the heat exchange time, resulting in a decrease in temperature difference. In addition, at wind speeds of 1 m/s-1.5 m/s, the temperature difference remains above 2 ℃ after 8 hours.

3.3.4 Effect of the inlet air temperature

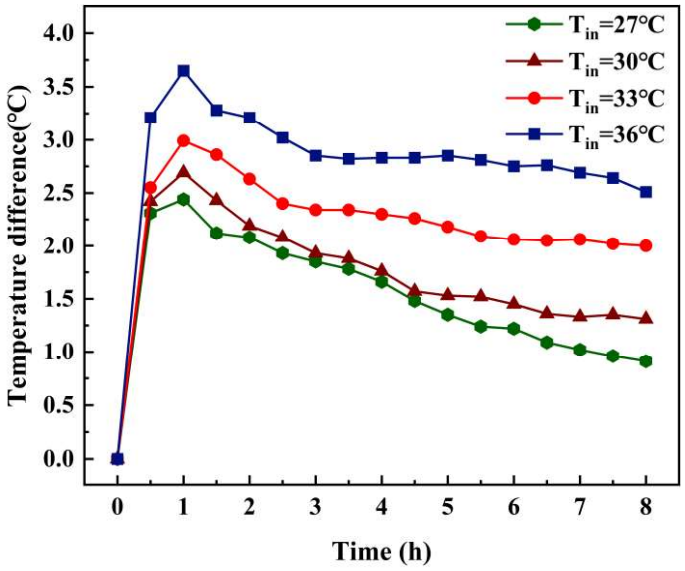


Fig. 17. Temperature difference at different inlet air temperatures.

Figure 17 shows the 8-hour temperature difference variation of the device placed without distance, with the air velocity of 1.5 m/s and the aperture size of 10 cm at different inlet air temperature. The higher the inlet air temperature, the more significant the temperature difference. It can be observed that as time passes, the temperature difference begins to decrease after reaching its maximum value within one hour. This is because the air with increased inlet air temperature has higher thermal energy, and the cooling capacity is related to the temperature difference between heat

exchange. As the heat absorbed by PCM increases, the temperature difference between air and PPCP decreases, resulting in a decrease in cooling capacity, and the temperature difference gradually decreases. The graph shows that at four different temperatures, the average temperature difference within 8 hours is 1.52 ℃ to 2.92 ℃. When the inlet air temperature is 36 ℃, the maximum temperature difference reaches 3.65 ℃.

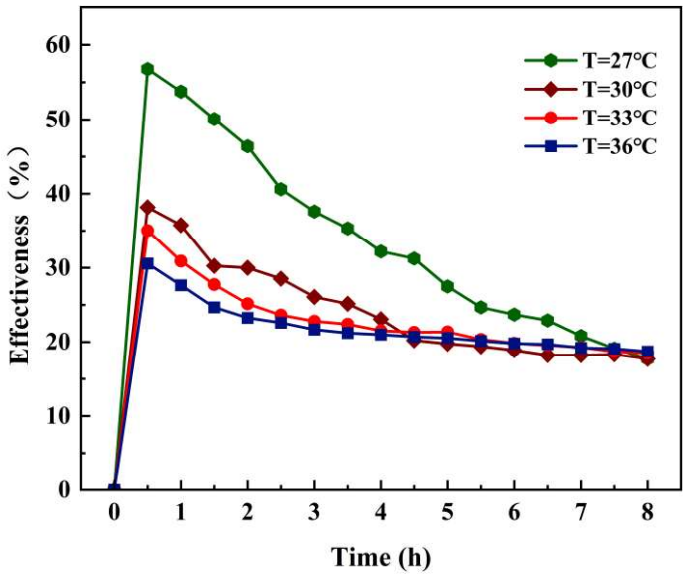


Fig. 18. Effectiveness of the device at different temperatures.

Figure 18 shows the effectiveness of the device, which indicates the thermal performance of the equipment relative to its maximum cooling potential. The effect depends on the air temperature at the inlet and outlet of the device, as well as the initial temperature of the system. The denominator in formula (6) represents the maximum temperature drop potential that the system can theoretically achieve. When the inlet air temperature is elevated, despite the actual temperature drop, temperature difference may increase, but the maximum temperature drop potential of the system will increase at a faster rate. So, the higher the temperature, the lower the effect. As shown in the figure, when the inlet air temperature is 27 ℃, the PCHD achieves optimal thermal performance, with an average effectiveness of 42.96% within 8 hours. As the temperature increases, the maximum cooling potential thermal performance of PCHD gradually decreases but remains above 20% within 8 hours.

4 Discussion

4.1 Comprehensive analysis

In air conditioning systems, the addition of phase change heat exchange components has made the configuration and performance effects of PCHD a key focus of research. The study used extreme value analysis to investigate the influence of inlet air temperature, air velocity, the aperture size, and the placement distance. As shown in Table 6, the K_i value represents the total sum of three experimental results for a factor at the same level. The k value reflects the average effect at this level, and the average value of the K_i values ($k_i = K_i/3$). The R value is used to measure the impact size of a factor on experimental results, calculated as $R=k_{max}-k_{min}$. The R value represents $R_T>R_V>R_A>R_D$, which means that the primary and secondary factors affecting the temperature difference of PCHD are inlet air temperature > air velocity >aperture size of PPCPs > placement distance of PPCPs. The analysis shows that the inlet air temperature has the greatest impact on equipment performance. Additionally, the optimal configuration for PCHD is the air velocity of 1.5 m/s, the aperture size of 6 cm, and the placement distance of 10 cm.

Table 6
Range analysis.

Case	Inlet air temperature (°C)	Velocity (m/s)	Aperture (cm)	Distance (cm)	Temperature difference (°C)
12	30	1.5	10	0	1.80
13	33	2.5	10	5	2.08
14	36	2	10	10	2.98
15	36	2.5	8	0	3.58
16	30	2.0	8	5	1.65
17	33	1.5	8	10	2.74
18	33	2	6	0	2.51
19	36	1.5	6	5	3.90
20	30	2.5	6	10	1.77
K_1	5.50	8.54	8.18	7.49	
K_2	7.28	7.32	7.95	7.76	
K_3	10.26	7.18	6.91	7.79	
$k_1=（K_1/3）$	1.83	2.85	2.73	2.50	
$k_2=（K_2/3）$	2.43	2.44	2.65	2.59	
$k_3=（K_3/3）$	3.42	2.39	2.30	2.60	
R	1.59	0.45	0.42	0.10	

Based on the analysis of the results, the impact of inlet air temperature on PCHD is the most significant, the higher the inlet air temperature, the greater the temperature difference. Therefore, as illustrated in figure 19, when planning the layout of the heat exchange function in the air conditioning system, it should be placed before the cooling function. This ensures that untreated fresh air undergoes heat exchange with PCHD before entering the system. After a certain temperature reduction, dust removal, dehumidification and cooling treatment are conducted to meet the air supply requirements. After PCHD treatment, the air temperature decreases, reducing the demand for mechanical cooling load, thus reducing the energy consumption of mechanical cooling, and improving energy efficiency.

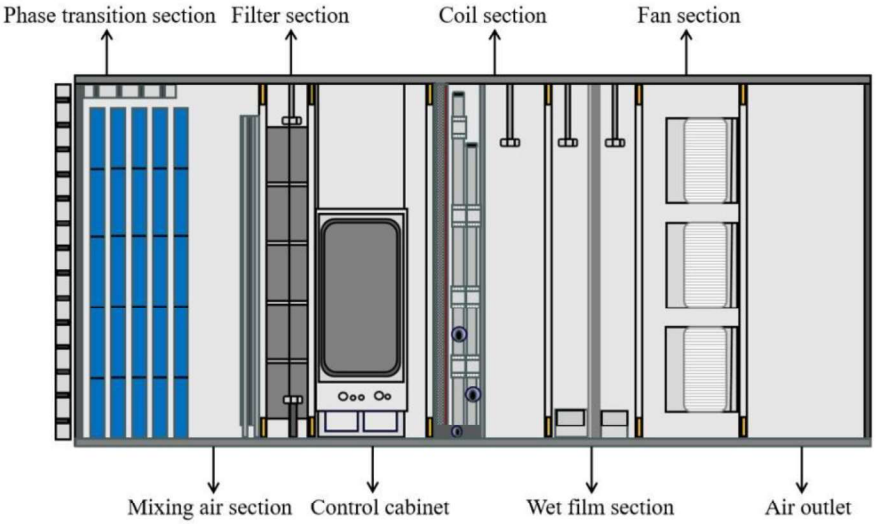


Fig. 19. Schematic diagram of the function section of air conditioning system.

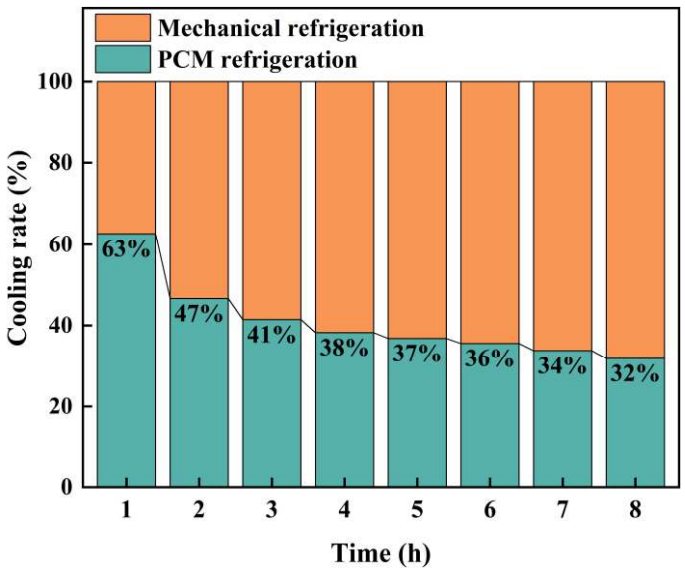
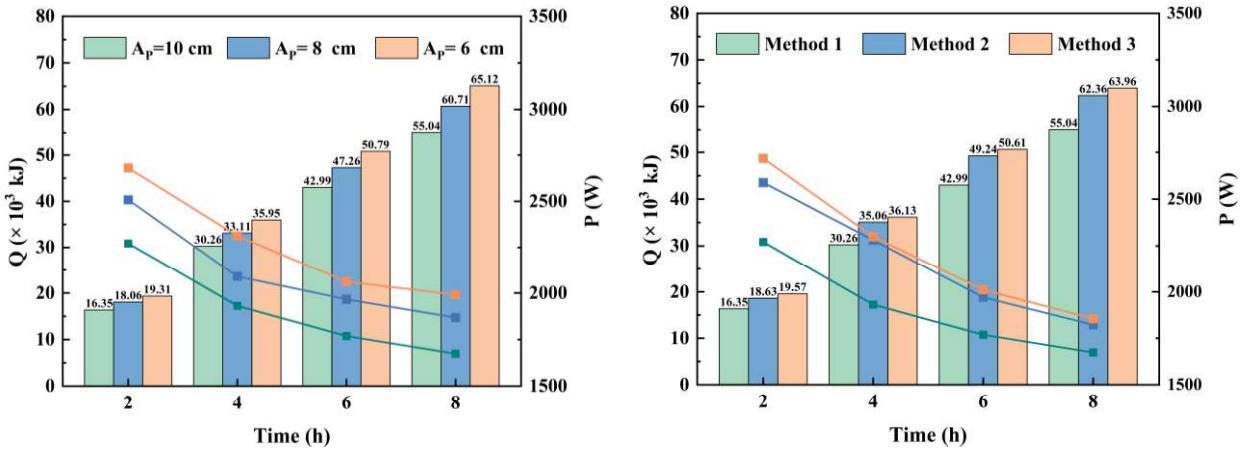


Fig. 20. The proportion of phase change refrigeration and mechanical refrigeration in 8 hours.

Figure 20 shows the proportion of energy savings achieved by phase change cooling over 8 hours under case 3 conditions for PCHD. As time progresses, the proportion of energy savings gradually decreases. In the initial stage, phase change cooling, when used in conjunction with mechanical cooling, can save 63% of energy. After 8 hours, phase change cooling alone maintains 32% energy savings. Throughout the process, it can help save a total of 41% of energy. PCHD demonstrates excellent performance in enhancing energy efficiency and reducing emissions.

4.2 Energy efficiency and economy of the PCHD assisted air conditioner



(a) (b)

Fig. 21. Cooling power and cooling capacity of the PCHD :(a) Under different aperture sizes. (b)Under different placement distances.

Figure 21 (a) shows the differences in cooling power and heat absorption of PPCPs with three different aperture sizes. Under the same conditions, reducing the aperture size by 2 cm can increase the cooling capacity by about 5% within 8 hours. The cooling capacity of 6 cm hole PPCP reaches 65.12 × 10³ kJ. (b) shows the differences in cooling power and heat absorption of PPCPs placed at three different distances. Within 8 hours, the average cooling power of the three placement distances are 1911.13, 2165.40 W, and 2220.97 W, respectively, with cooling capacities of 55.04 × 10³ kJ, 62.36 × 10³ kJ, and 63.96 × 10³ kJ.

COP value refers to the energy efficiency level of the system in the refrigeration mode. For this

system, the input power comes from the operation of the fan, and the input power P_w is obtained from the fan parameters provided by the supplier. The energy efficiency level of the system is analyzed as shown in Table 7.

Table 7

Energy efficiency analysis under different air velocities

Air volume(m^3/h)	Time (h)	P_w (W)	P (W)	COP
1521	8	320	1328.29	4.15
2282	8	360	1911.12	5.31
3042	8	400	2226.98	5.57
3803	8	440	2506.64	5.69

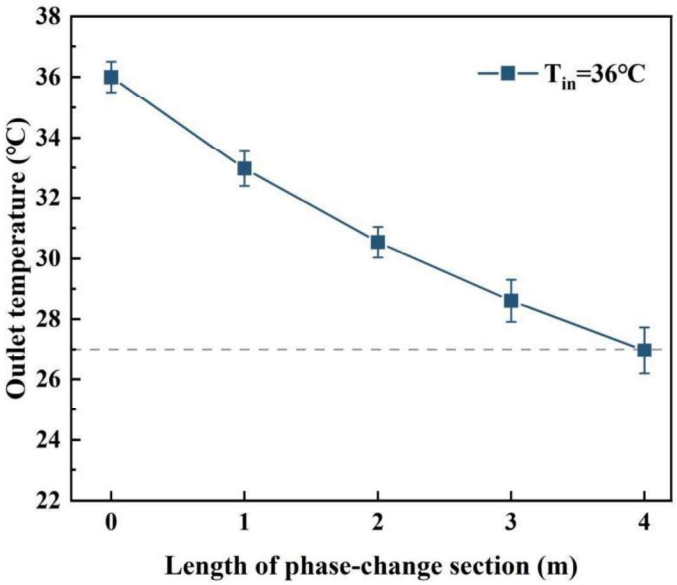


Fig. 22. Variation of outlet temperature with the PCHD length.

Figure 22 shows the variation of outlet temperature with the PCHD length. According to ASHRAE TC 9.9, the maximum recommended supply air temperature for data centers is 27 ℃. As shown in the figure, the inlet air temperature is 36 °C, and the outlet temperature decreases as the length of the PCHD increases, and when the length is increased to 4 meters, the outlet temperature decreases to 27 °C, which meets the requirement of air supply.

Table 8

Economics analysis

Materials	Unit	Unit price	Quantities	Amount
Encapsulation structure	m^2	130	48.32	￥6281.6
PCM	kg	25	900	￥22500
Labor costs	pcs	200	20	￥4000
Subtotal			￥32781.6	

According to the research findings, Table 8 provides an economic analysis of the PCHD. The table illustrates that the total investment for the 4 meter PPCPs is￥32781.6. Since phase change heat exchange occurs spontaneously with the ambient temperature difference, it avoids the provision of high-energy electricity and has a low risk of component failure and wear, greatly reducing equipment maintenance and operating costs. Compared with the traditional air conditioning system, which has the characteristics of complex components, difficult installation and complicated maintenance, this equipment has the advantages of easy installation and simple maintenance. At the same time, in terms

of operation, it greatly reduces the dependence on electric drive, showing good sustainability and high implementation feasibility.

4.3 Comparison analysis

As shown in Table 9, Zheng et al. [48] designed a shell-and-tube phase change heat storage device and studied the effects of different flow rates and temperatures on the temperature distribution, heat, power, and efficiency of PCMs during melting and solidification by experiments. Lu et al.[52] investigated the thermal performance of vertical multi-shell and spiral finned tube devices and evaluated the thermal charge-discharge characteristics, heat storage and discharge, average charge-discharge power, total charge-discharge time, and instantaneous efficiency of the device. Mahdi et al. [53] used lauric acid and water as PCMs to conduct theoretical simulations and experimental validations of latent heat storage and evaluated the time-dependent PCM simulation of liquid phase fraction, temperature, and storage power. Yang et al. [33] proposed a novel design for a phase change ventilation device and studied the charge and discharge process of the device and conducted experimental studies on the influence of inlet air temperature, inlet speed, number, and thickness of phase change plate on the performance. Lin et al.[54] suggested filling annular tubes with wax/expanded graphite composite materials as PCMs to enhance the performance of heat exchangers. Through comparative analysis of existing packaging configurations, this study develops a novel porous plate heat exchanger. Experimental results demonstrate a threefold enhancement in heat transfer capacity compared to conventional plate designs, while requiring only 25% additional packaging material within similar spatial constraints. This improvement contributes to both higher energy efficiency and lower mechanical refrigeration requirements.

Table9

Comparison analysis.

Related research	PCM	Material usage (L)	Time (h)	Heat storage (kJ)
Zheng et al. [48]	paraffin	593		8.10×10^4
Lu et al.[52]	paraffin	21.24	2.5	6.00×10^3
Mahdi et al. [53]	Lauric acid、water	7.66	0.4	6.48×10^2
Yang et al. [33]	paraffin	204	8	2.19×10^4
Lin et al.[54]	paraffin		2	4.68×10^2
Current work	paraffin	255	8	6.58×10^4

4.4 Future work

This paper studies the cooling performance of the air for PCHD under different working conditions. It is found that when PPCP is placed at intervals, the temperature change of PCM in each plate is different, which is due to the fact that the air passes through each PPCP and the temperature decreases to a certain extent, and the temperature difference between PCM and air in different positions of PPCP is different. Therefore, the corresponding phase transition temperature gradient can be designed in subsequent studies considering the temperature difference when air passes through each PPCP. The device can be divided into front, middle, and rear sections, and graded according to the phase change temperature range of the PCM to ensure that the PCM in each module of the PPCP remains within the optimal phase change temperature range. At the same time, an evaporative cooling device can be added in the gap space of the PCHD, combining phase change energy storage

technology with evaporative cooling technology, thereby improving the utilization of phase change inside the device and enhancing its cooling performance.

Furthermore, Yang et al. [55] integrated auxiliary technologies with the cooling system to flexibly switch between mechanical cooling, partial free cooling, and full free cooling modes based on environmental temperature changes, thus achieving a hybrid cooling source operation. This approach allows for the combination of natural cooling, phase change cooling, and mechanical cooling, prioritizing natural and phase change cooling to reduce the need for mechanical cooling, thereby enhancing energy efficiency, and reducing carbon emissions.

5 Conclusion

Based on the internal structure of air conditioning systems and the climate characteristics of Gui'an District in Guizhou Province, this study combines the features of plate heat exchangers and shell-and-tube heat exchangers. It examines a phase change heat exchanger suitable for use within air conditioning systems, analyzing factors such as inlet air temperature, air supply speed, the size of the PPCP holes, and installation methods affect the performance of the PCHD. The main conclusions of this study are as follows:

(1) The PCHD can reduce the air temperature by an average of 1.59 to 3.90 ℃ within 8 hours.

(2) The aperture size of the PPCP has a significant effect on its cooling performance; reducing the aperture size by 2 cm improves the cooling performance by 8% to 11%.

(3) In a comprehensive analysis of multiple factors, the primary and secondary factors affecting the performance of the PCHD are inlet air temperature, air velocity, the aperture size, and the placement distance.

(4) During high-temperature loads, the PCHD can assist in reducing mechanical energy consumption by up to 63%.

CRediT authorship contribution statement

Zhongqiu Wang: Writing – original draft, Software, Methodology, Investigation, Formal analysis, Data curation. **Zujing Zhang:** Writing – review & editing, Project administration, Methodology, Funding acquisition, Data curation. **Ruiyong Mao:** Writing – review & editing, Methodology. **Xing Liang:** Writing – review & editing, Methodology. **Jiri Zhou:** Project administration, Funding acquisition. **Hongwei Wu:** Writing – review & editing, Methodology.

Declaration of Competing Interest

We declare that we have no financial and personal relationships with other people or organizations that can inappropriately influence our work, there is no professional or other personal interest of any nature or kind in any product, service and/or company that could be construed as influencing the position presented in, or the review of, the manuscript entitled ***'Experimental study on thermal performance of porous phase change plates assisted air conditioning system in data centers'***.

Acknowledgments

The author would like to thank the financial support of the National Natural Science Foundation of China (NO.52168013), the Guizhou Provincial Science and Technology Projects (NO. ZK [2022]151) and the Guizhou Province Postgraduate Research Fund Project (NO. 2024YJSKYJJ114).

References

[1] N. Lei, M. Ganeshalingam, E. Masanet, S. Smith, A. Shehabi. Shedding light on U.S. small and midsize data centers: Exploring insights from the CBECS survey. Energy and Buildings. 339 (2025) 115734.
[2] N. Wang, Y. Guo, H. Yu, S. Shao. Investigation on performance enhancement of micro-channel separated heat pipe in data center: A coupled heat-mass-flow characterization approach. Applied Thermal Engineering. 248 (2024) 123327.
[3] R.F. Mansour, H. Alhumyani, S.A. Khalek, R.A. Saeed, D. Gupta. Design of cultural emperor penguin optimizer for energy-efficient resource scheduling in green cloud computing environment. Cluster Computing. 26 (2023) 575-86.
[4] J. Cho, Y. Kim. Development of modular air containment system: Thermal performance optimization of row-based cooling for high-density data centers. Energy. 231 (2021) 120838.
[5] Y. Ichinose, M. Hayashi, S. Nomura, B. Moser, K. Hiekata. Sustainable Data Centers in Southeast Asia: Offshore, Nearshore, and Onshore Systems for Integrated Data and Power. Sustainable Cities and Society. 81 (2022) 103867.
[6] R. Bose, S. Roy, H. Mondal, D.R. Chowdhury, S. Chakraborty. Energy-efficient approach to lower the carbon emissions of data centers. Computing. 103 (2021) 1703-21.
[7] X. Ma, Q. Zhang, S. Zou. An experimental and numerical study on the thermal performance of a loop thermosyphon integrated with latent thermal energy storage for emergency cooling in a data center. Energy. 253 (2022) 123946.
[8] C. Zhang, B. Hou, M. Li, C. Dang, X. Chen, X. Li, et al. Feasibility analysis of multi-mode data center liquid cooling system integrated with Carnot battery energy storage module. Energy. 320 (2025) 135385.
[9] M. Sermsuk, Y. Sukjai, M. Wiboonrat, K. Kiatkittipong. Feasibility study of a combined system of electricity generation and cooling from liquefied natural gas to reduce the electricity cost of data centres. Energy. 254 (2022) 124397.
[10] J. Wang, Y. Tian, Z. Qi, L. Zeng, P. Wang, S. Yoon. Sensor fault diagnosis and correction for data center cooling system using hybrid multi-label random Forest and Bayesian Inference. Building and Environment. 249 (2024) 111124.
[11] R. Tu, Y. Ge, X. Chang, L. Liu, X. Yang. Performance Analyses of a novel operation strategy for data Centre's centralized Water-Cooling system to match personalized cooling demands. Applied Thermal Engineering. 273 (2025) 126553.
[12] C. Koronen, M. Åhman, L.J. Nilsson. Data centres in future European energy systems—energy efficiency, integration and policy. Energy Efficiency. 13 (2020) 129-44.
[13] F. Zhou, W. Gu, G. Ma. Advancements in data center cooling systems: From refrigeration to high performance cooling. Energy and Buildings. 320 (2024) 114634.
[14] A.A. Alkrush, M.S. Salem, O. Abdelrehim, A.A. Hegazi. Data centers cooling: A critical review of techniques, challenges, and energy saving solutions. International Journal of Refrigeration. 160

(2024) 246-62.
[15] Y. Jin, X. Bai, X. Xu, R. Mi, Z. Li. Climate zones for the application of water-side economizer in a data center cooling system. Applied Thermal Engineering. 250 (2024) 123450.
[16] P.M. Wenzel, M. Mühlen, P. Radgen. Free Cooling for Saving Energy: Technical Market Analysis of Dry, Wet, and Hybrid Cooling Based on Manufacturer Data. Energies. 16 (2023) 3661.
[17] W. He, J. Zhang, H. Li, S. Liu, Y. Wang, B. Lv, et al. Optimal thermal management of server cooling system based cooling tower under different ambient temperatures. Applied Thermal Engineering. 207 (2022) 118176.
[18] G.D. Chethana, B. Sadashive Gowda. Thermal management of air and liquid cooled data centres: A review. Materials Today: Proceedings. 45 (2021) 145-9.
[19] M. Kuzay, A. Dogan, S. Yilmaz, O. Herkiloglu, A.S. Atalay, A. Cemberci, et al. Retrofitting of an air-cooled data center for energy efficiency. Case Studies in Thermal Engineering. 36 (2022) 102228.
[20] L. Silva-Llanca, C. Ponce, E. Bermúdez, D. Martínez, A.J. Díaz, F. Aguirre. Improving energy and water consumption of a data center via air free-cooling economization: The effect weather on its performance. Energy Conversion and Management. 292 (2023) 117344.
[21] M.H. Jahangir, R. Mokhtari, S.A. Mousavi. Performance evaluation and financial analysis of applying hybrid renewable systems in cooling unit of data centers – A case study. Sustainable Energy Technologies and Assessments. 46 (2021) 101220.
[22] D. Chen, Y. Ma, L. Wang, M. Yao. Spatio-temporal management of renewable energy consumption, carbon emissions, and cost in data centers. Sustainable Computing: Informatics and Systems. 41 (2024) 100950.
[23] M.A. Basit, S. Dilshad, R. Badar, S.M. Sami ur Rehman. Limitations, challenges, and solution approaches in grid-connected renewable energy systems. International Journal of Energy Research. 44 (2020) 4132-62.
[24] M.M. Rahman, A.O. Oni, E. Gemechu, A. Kumar. Assessment of energy storage technologies: A review. Energy Conversion and Management. 223 (2020) 113295.
[25] L. Liu, Q. Zhang, Z. Zhai, C. Yue, X. Ma. State-of-the-art on thermal energy storage technologies in data center. Energy and Buildings. 226 (2020) 110345.
[26] Y. Zhu, G. Englmair, H. Huang, J. Dragsted, Y. Yuan, J. Fan, et al. Numerical investigations of a latent thermal energy storage for data center cooling. Applied Thermal Engineering. 236 (2024) 121598.
[27] B. Kurşun, M. Balta, F. Polat. Simultaneous evaluation of charge/discharge times and energy storage/release capacities in multi-tube latent heat energy storage with metal foam-enhanced PCM. Journal of Energy Storage. 108 (2025) 115090.
[28] Y. Xie, J. Liu, W. Ma, J. Sheng, P. Zhang. Review of the heat transfer enhancement for phase change heat storage devices. Journal of Energy Storage. 86 (2024) 111336.
[29] W. Li, Y. Liang, H. Gao, R. Li, Y. Guo, L. Yang. Development and experimental analysis of a novel type of phase change material based shell-and-tube latent heat storage for heat pump system. Energy Conversion and Management. 321 (2024) 119095.
[30] Q. Wu, J. Wang, X. Meng. Influence of wall thermal performance on the contribution efficiency of the Phase-Change Material (PCM) layer. Case Studies in Thermal Engineering. 28 (2021) 101398.
[31] B. Huang, Z. Zheng, G. Lu, X. Zhai. Design and experimental investigation of a PCM based cooling storage unit for emergency cooling in data center. Energy and Buildings. 259 (2022) 111871.
[32] Y. Yan, Z. Liu, L. Zeng, W. Li, H. Yang, H. Gao. Evaluation of the heat transfer and energy efficiency of a solar phase change heat storage system with a novel heat transfer structure. Energy

Conversion and Management. 340 (2025) 120000.
[33] L. Yang, H. Wu, Z. Zhang, R. Mao, J. Zhou, X. Liang. Experimental investigation on application potential of phase change assisted direct ventilation cooling system for Gui'an data center. Applied Thermal Engineering. 254 (2024) 123932.
[34] X. Yi, H. Xu, R. Mao, H. Wu, X. Gao, J. Zhou, et al. Experimental investigation on evaporative cooling coupled phase change energy storage technology for data centers under natural air cooling. International Communications in Heat and Mass Transfer. 159 (2024) 108127.
[35] Z. Zheng, B. Huang, G. Lu, X. Zhai. Design and optimization of an air-based phase change cold storage unit through cascaded construction for emergency cooling in IDC. Energy. 241 (2022) 122897.
[36] J. Wang, Z. Shao, J. Du, F. Chen, Z. Song. Effects of inlet and outlet configurations on the topological optimization design of cooling plates for lithium-ion batteries. Journal of Energy Storage. 79 (2024) 110124.
[37] J. Wang, F. Chen, Z. Shao, L. He. Study of the influence of objective functions on the topology optimization design of battery cold plate. Applied Thermal Engineering. 226 (2023) 120326.
[38] F. Chen, J. Wang, X. Yang. Topology optimization design and numerical analysis on cold plates for lithium-ion battery thermal management. International Journal of Heat and Mass Transfer. 183 (2022) 122087.
[39] İ.G. Demirkıran, K. Niedermeier, E. Çetkin. Hollowed and perforated fins in latent heat storage units for High-Temperature hybrid thermal energy storage applications. Energy Conversion and Management. 340 (2025) 119998.
[40] X. Li, Z. Zhang, R. Mao, X. Liang, J. Zhou, H. Wu. Experimental investigation on thermal performance of phase change plates used in hot and humid environment with ventilation. Journal of Building Engineering. 104 (2025) 112420.
[41] R. Ahmadi, M.J. Hosseini, A.A. Ranjbar, R. Bahrampoury. Phase change in spiral coil heat storage systems. Sustainable Cities and Society. 38 (2018) 145-57.
[42] G. Gioanola, H. Bastida, E. Guelpa, V. Verda, A. Sciacovelli. Innovative methodology for optimized design and thermo-economic analysis of pillow-plate latent heat thermal energy storage: a case study on heat recovery in the brewing industry. Energy Conversion and Management. 341 (2025) 120025.
[43] C. Zhang, J. Li, Y. Chen. Improving the energy discharging performance of a latent heat storage (LHS) unit using fractal-tree-shaped fins. Applied Energy. 259 (2020) 114102.
[44] S.R. Chalivendula, H. Tarigonda. Recent Advances in Organic Phase Change Materials for Thermal Energy Storage: A Review on Sustainable Development Applications. International Journal of Thermophysics. 46 (2025) 88.
[45] Z. Leng, Y. Yuan, X. Cao, J. Wang, F. Haghighat. Melting and solidification performance in two horizontal shell-and-tube heat exchangers with different structures. International Journal of Energy Research. 44 (2020) 11288-301.
[46] A. Rahmani, M. Dibaj, M. Akrami. Enhancing Heat Storage Cooling Systems via the Implementation of Honeycomb-Inspired Design: Investigating Efficiency and Performance. Energies. 17 (2024) 351.
[47] J.N.W. Chiu, V. Martin. Multistage latent heat cold thermal energy storage design analysis. Applied Energy. 112 (2013) 1438-45.
[48] W. Zheng, S. Yang, W. Li, M. Luo, C. Song, Y. Zhang. Experimental study on thermal performance of phase change heat storage device with rectangular shell structure. Applied Thermal Engineering. 214 (2022) 118897.
[49] E. Akyol, O. Hacıhafızoğlu, Ç. Susantez, K. Kahveci, U. Akyol. Experimental and numerical

investigation of heat transfer in a channel with multiple phase change materials (PCMs). Journal of Energy Storage. 45 (2022) 103710.
[50] Z. Han, H. Wei, X. Sun, C. Bai, D. Xue, X. Li. Study on influence of operating parameters of data center air conditioning system based on the concept of on-demand cooling. Renewable Energy. 160 (2020) 99-111.
[51] D. Zhou, C.Y. Zhao. Experimental investigations on heat transfer in phase change materials (PCMs) embedded in porous materials. Applied Thermal Engineering. 31 (2011) 970-7.
[52] B. Lu, Y. Zhang, D. Sun, Z. Yuan, S. Yang. Experimental investigation on thermal behavior of paraffin in a vertical shell and spiral fin tube latent heat thermal energy storage unit. Applied Thermal Engineering. 187 (2021) 116575.
[53] M.S. Mahdi, H.B. Mahood, A.A. Khadom, A.N. Campbell. Numerical simulations and experimental verification of the thermal performance of phase change materials in a tube-bundle latent heat thermal energy storage system. Applied Thermal Engineering. 194 (2021) 117079.
[54] W. Lin, R. Huang, X. Fang, Z. Zhang. Improvement of thermal performance of novel heat exchanger with latent heat storage. International Journal of Heat and Mass Transfer. 140 (2019) 877-85.
[55] Y. Yang, B. Wang, Q. Zhou. Energy Saving Analysis of Free Cooling System in the Data Center. Procedia Engineering. 205 (2017) 1815-9.